FEBS 29293 FEBS Letters 579 (2005) 1389–1393

Discovery of quinazolinone and quinoxaline derivatives as potent and selective poly(ADP-ribose) polymerase-1/2 inhibitors

Akinori Iwashita[a,*], Kouji Hattori[b,*], Hirofumi Yamamoto[b], Junya Ishida[b], Yoshiyuki Kido[b], Kazunori Kamijo[b], Kenji Murano[b], Hiroshi Miyake[b], Takayoshi Kinoshita[c], Masaichi Warizaya[c], Mitsuru Ohkubo[c], Nobuya Matsuoka[a], Seitaro Mutoh[a]

[a] *Medicinal Biology Research Laboratories, Fujisawa Pharmaceutical Co., Ltd., 2-1-6 Kashima, Yodogawa-ku, Osaka 532-8514, Japan*
[b] *Medicinal Chemistry Research Laboratories, Fujisawa Pharmaceutical Co., Ltd., 2-1-6 Kashima, Yodogawa-ku, Osaka 532-8514, Japan*
[c] *Exploratory Research Laboratories, 5-2-3, Tokodai, Tsukuba, Ibaraki 300-2698, Japan*

Received 3 January 2005; revised 17 January 2005; accepted 17 January 2005

Available online 29 January 2005

Edited by Hans Eklund

Abstract **Two classes of quinazolinone derivatives and quinoxaline derivatives were identified as potent and selective poly(ADP-ribose) polymerase-1 and 2 (PARP-1) and (PARP-2) inhibitors, respectively. In PARP enzyme assays using recombinant PARP-1 and PARP-2, quinazolinone derivatives displayed relatively high selectivity for PARP-1 and quinoxaline derivatives showed superior selectivity for PARP-2. SBDD analysis via a combination of X-ray structural study and homology modeling suggested distinct interactions of inhibitors with PARP-1 and PARP-2. These findings provide a new structural framework for the design of selective inhibitors for PARP-1 and PARP-2.**

Keywords: Poly(ADP-ribose) polymerase-1; Poly(ADP-ribose) polymerase-2; SBDD

1. Introduction

Poly(ADP-ribose) polymerase (PARP) is an abundant nuclear enzyme in eukaryotic cells that has been implicated to become activated in response to DNA damage. Activated PARP catalyzes the transfer of ADP-ribose units from nicotinamide adenine dinucleotide (NAD^+) to nuclear acceptor proteins such as histones, topoisomerases, DNA polymerases, DNA ligases and PARP itself. Excessive activation of PARP consumes NAD^+ and consequently ATP, culminating in cell dysfunction or necrosis. Furthermore, PARP has also been implicated in a caspase-independent apoptosis pathway mediated by apoptosis-inducing factor [1]. PARP inhibitors provided remarkable protection from tissue damage in various forms of reperfusion injury, inflammation and neurotoxicity in animal models [2]. Thus, inhibition of PARP by pharmacological agents could be useful in the treatment of inflammatory disease, neurodegenerative disease and several other diseases involved in PARP activation.

Characterized family members of PARP currently include the proteins PARP-1, PARP-2, PARP-3, Tankyrase-1, Tankyrase-2, TiPARP and vPARP. Although PARP-1 has been believed to be responsible for all the DNA-damage dependent poly(ADP-ribose) (PAR) synthesis in mammalian cells, a novel DNA-damage dependent PARP-2 was subsequently discovered as a result of the presence of residual DNA-dependent PARP activity in embryonic fibroblasts derived from PARP-1-deficient mice [3,4]. PARP-1 and PARP-2 are structurally different from each other, but they share a DNA-binding domain and the catalytic domain of PARP-2 has high resemblance to that of PARP-1. The first crystal structure available was that of the catalytic domain of chicken PARP-1, which informed of the binding mode of inhibitors to the NAD^+ binding site [5]. Recently, the second crystal structure of murine PARP-2 has been solved. The catalytic domain of murine PARP-2 is found to be very similar to that of PARP-1 [6]. Furthermore, it has been reported that the PARP catalytic domain shows the highest degree of homology between different species [7,8], suggesting that PARP inhibitors may have no species-difference in terms of inhibitory activity among human, rat and mouse PARPs [9].

Over the last two decades, a large number of PARP-1 inhibitors have been developed [10], the majority of which mimic to some degree the nicotinamide moiety of NAD^+ and bind to the donor site of the protein. However, the residues in the donor site of PARP-1 that provide hydrogen-bonding interactions with these inhibitors are completely conserved in PARP-2, suggesting that these existing PARP-1 inhibitors would not discriminate between PARP-1 and PARP-2 [6]. We have recently discovered two classes of quinazolinone structure and quinoxaline structure as potent and brain penetrable PARP-1 inhibitors which can represent an attractive therapeutic candidate for neurodegenerative disorders such as cerebral ischemia or Parkinson's disease [11]. In this paper, we describe our extensive research on PARP-1/2 selective inhibitors which discriminate between PARP-1 and PARP-2 using SBDD analysis by a combination of X-ray analysis and homology modeling.

*Corresponding authors. Fax: +81 6 6304 5435.
E-mail addresses: aki_iwashita@po.fujisawa.co.jp (A. Iwashita), kouji_hattori@po.fujisawa.co.jp (K. Hattori).

Abbreviations: PARP-1, Poly(ADP-ribose) polymerase-1; PARP-2, Poly(ADP-ribose) polymerase-2 (PARP-2); NAD^+, nicotinamide adenine dinucleotide; PAR, Poly(ADP-ribose); NI site, nicotinamide-ribose binding site; AD site, adenine-ribose binding site

0014-5793/$30.00
doi:10.1016/j.febslet.2005.01.036

2. Materials and methods

2.1. Materials

Recombinant human PARP enzyme was purchased from Trevigen, Inc. (Gaithersburg, MD) and recombinant mouse PARP-1 and PARP-2 enzymes were purchased from Alexis Biochemicals (San Diego, CA). Unless otherwise stated, all other chemicals were purchased from Sigma–Aldrich (St. Louis, MO).

2.2. PARP assay

To assess the inhibitory activity of novel inhibitors, the PARP enzyme assay was carried out in a final volume of 100 μl consisting of 50 mM Tris–HCl (pH 8.0), 25 mM $MgCl_2$, 1 mM dithiothreitol, 10 μg activated salmon testes DNA, 0.1 μCi of [adenylate-^{32}P]-NAD, 0.2 units of recombinant human PARP-1, recombinant mouse PARP-1 or PARP-2, and various concentrations of PARP inhibitors. The reaction mixture was incubated at room temperature (23 °C) for 15 min, and the reaction was terminated by adding 200 μl of ice cold 20% trichloroacetic acid (TCA) and incubated at 4 °C for 10 min. The precipitate was transferred onto GF/B filter (Packard Unifilter-GF/B) and washed three times with 10% TCA solution and 70% ethanol. After the filter was dried, the radioactivity was determined by liquid scintillation counting. IC_{50} values were calculated from the concentration dependence of the inhibition curves by using computer-assisted non-linear regression analyses.

2.3. X-ray crystallography of *10*/*PARP-1*

The C-terminal catalytic domain of PARP (catPARP) from human was purified as described previously [12]. Crystals of catPARP complexed with **10** were obtained by the sitting drop vapor-diffusion method, adding equal volumes of concentrated protein solution (20 mg/ml) and a crystallization buffer (2.2–2.3 M $(NH_4)_2SO_4$, 1% v/v PEG400 and 100 mM Tris–HCl, pH 8.0) at 3:1 molar ratio of **10** to protein. The crystal was transferred to cryo-protectant oil, Paratone-N (Hampton Research) and flash-cooled in a liquid N_2 stream at 100 K and X-ray diffraction data was collected at SPring8/BL32B2, using a R-Axis V imaging plate detector (Rigaku). The crystal formed in space group $P2_1$ with unit cell parameters, $a = 90.05$ Å, $b = 77.08$ Å, $c = 113.72$ Å, $\beta = 117.43°$. The data was processed and scaled using the program *Crystal Clear* (Rigaku) at resolution range of 29.25–3.0 Å with overall R_{merge} and completeness of 8.5% and 94.0%, respectively, against 26 413 unique reflections out of 107 770 observations. Each asymmetric unit contained four protein molecules with solvent content of 46.0%. The monomer structure of catPARP (PDB code: 1UK0) [8] was used as the initial model for molecular replacement with the program *AMoRe* in the *CCP4* package [13]. The resulting model showed four distinct solutions and yielded a correlation coefficient of 59.0% and *R*-factor of 43.9% through a combination of the solutions. The tetrameric structure was subsequently refined with rigid body, simulated annealing, position and restrained B-factor routine from the program *CNX* (Accelrys). The ligand could easily fit into the difference electron density map and was bound to all of the four protein molecules in the asymmetric unit with the same binding mode. After iterative cycles of refinement with position and restrained B-factor routine from the program *CNX* (Accelrys), and manual model improvement with the program *QUANTA* (Accelrys), the final model yielded conventional and free R-factors of 23.3% and 28.8%, respectively, at a resolution range of 29.25–3.0 Å. The model coordinates have been deposited in the Protein Data Bank with the accession code 1WOK.

3. Results and discussion

3.1. SBDD study: quinazolinone structure

PARP-1/2 inhibitory activity of quinazolinone derivatives in vitro is outlined in Table 1. In general, the inhibitory potency of these derivatives was found to be largely dependent on the unique linker of the quinazolinone ring. Quinazolinone linked with a 4-phenyl-tetrahyropyridine moiety (**1**) exhibited strong potency against PARP-1 (IC_{50}: 21 nM), and exhibited an appropriately 30-fold less potency against PARP-2 (IC_{50}: 608 nM). The addition of a chloro group at the 8-position (**2**), which is important for bioavailability and brain penetration, resulted in almost the same activity and selectivity, while the addition of a chloro group at the 5-position (**6**) and a methyl group at the 8-position (**5**) showed 3 times lower selectivity than **1**. On the other hand, well-known inhibitors such as 2-methyl-4(3H)quinazolinone (**7**) and 3-AB (**8**) were less selective, with 0.6 and 0.9, respectively.

Fig. 1 shows the results of a structural study of the catalytic domain of human PARP-1 and PARP-2 complexes with the quinazolinone inhibitor **5** by X-ray analysis refined to 3.0 Å [8] and homology modeling by FAMS [14] based on the solved X-ray structure of murine PARP-2 [6]. As expected, there are no differences in the nicotinamide-ribose binding site (NI-site) between PARP-1 and PARP-2. The quinazolinone **5** binds to the NI site of PARP-2 by three hydrogen bonds (C═O to Ser446Oγ and Gly405NH; NH to Gly405C═O) and by a sandwiched hydrophobic interaction with the phenyl ring of Tyr438 and Tyr449 (Fig. 1B). We have reported that the design of the related quinazolinone analogue by modeling to allow a maximum fix of the 4-phenyl-tetrahydropyridine moiety to the adenine-ribose binding site (AD-site) of PARP-1. The terminal phenyl ring lies in a deep hydrophobic pocket which consists of the side chains of Leu769, Ile879, Pro881, and the methylene chain of Arg878 in PARP-1 (Fig. 1C). However, the critical difference between PARP-1 and PARP-2 in this hydrophobic pocket is the replacement of Leu769 in PARP-1, with Gly314 in PARP-2 (Fig. 1D). Based on these findings, it is clearly suggested that replacement of Leu769 by Gly314 leads to loss of a hydrophobic pocket and leads to a loss of potency against PARP-2. The change of only one amino acid is therefore sufficient to allow discrimination between PARP-1 and PARP-2.

3.2. SBDD study: quinoxaline structure

The SAR results of quinoxaline derivatives are outlined in Table 2. The activity of these inhibitors against PARP-2 is about 10-fold more potent than against PARP-1. Substitution at the *para* position of the terminal phenyl ring was more advantageous to activity than either *meta* or *ortho* substitution (data not shown). A twofold improvement in activity against PARP-2 was obtained by *p*-chloro (**10**) with $IC_{50} = 7.0$ nM and selectivity: 0.21.

To validate our results, we performed structural analysis by X-ray crystallography of human PARP-1 complexes with quinoxaline ligand and molecular modeling of PARP-2. Fig. 2A shows the structure of the human catalytic domain of PARP-1 complex with **10**, refined to 3.0 Å. The binding mode of human PARP-1 with **10** is almost the same as that of the previously disclosed benzimidazole analogues [15]. The carboxamide part of the inhibitor tightly binds to the same NI site by the three critical hydrogen bonds with Ser904 and Gly863 and the nitrogen of the quinoxaline ring binds to the carboxylic acid of Glu988, suggesting that this binding mode was conserved in PARP-2 (Fig. 2B). However, the main differences in the binding site of the terminal phenyl group of quinoxaline analogues within the groove could be used to introduce discrimination between PARP-1 and PARP-2. The Cl-phenyl group of **10** provides secondary contacts to the side chain of Asp766 formed by hydrogen bond with Tyr889, which replaces

Table 1
PARP-1/2 inhibitory activities of quinazolinone analogues

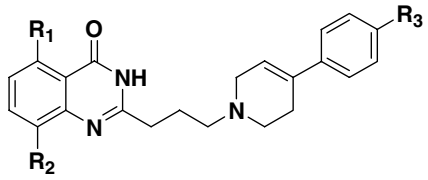

Compound	R_1	R_2	R_3	PARP-1 IC_{50} (nM)[a]	PARP-2 IC_{50} (nM)[a]	Selectivity PARP-2/1
1	H	H	H	21 ± 1.9	608 ± 12.9	29
2	H	Cl	H	23 ± 1.8	610 ± 18.1	27
3	H	Cl	CN	3.0 ± 0.6	87 ± 3.6	29
4	H	Cl	F	13 ± 1.3	500 ± 15.2	39
5	H	Me	F	16 ± 1.1	167 ± 25.7	10
6	Cl	H	H	68 ± 2.4	630 ± 28.5	9
7[b]				1200 ± 80	660 ± 24.7	0.6
8[c]				11200 ± 810	9810 ± 770	0.9

[a]The values are presented as means ± S.E. of three independent experiments (each experiment was triplicate).
[b]5-Chloro-2-methyl-4(3H)-quinazolinone.
[c]3-Aminobenzamide.

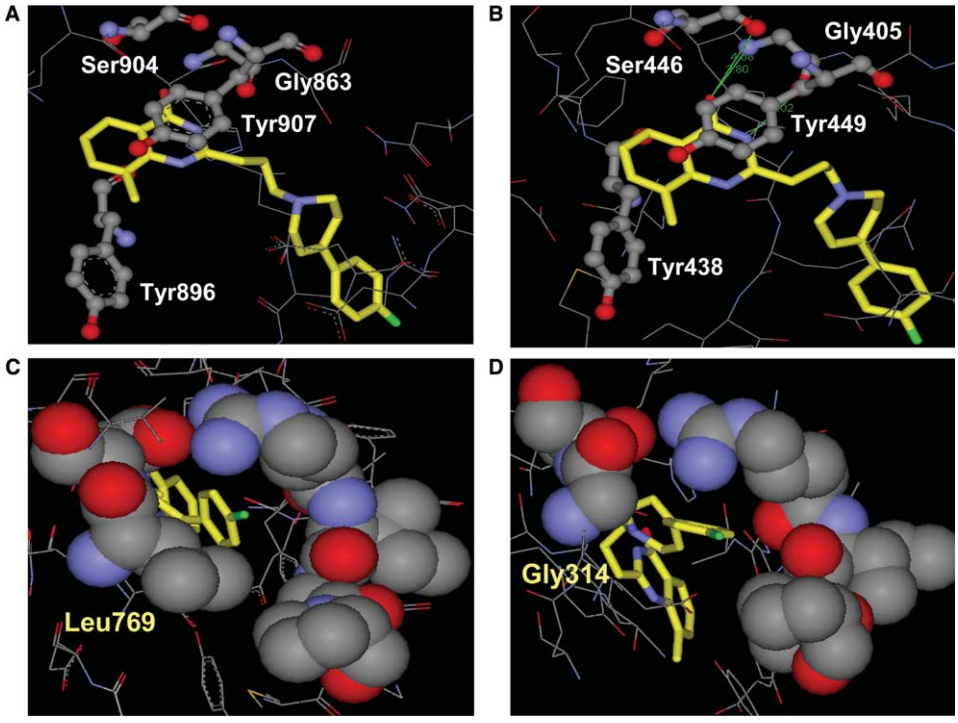

Fig. 1. (A) X-ray structure (3.0 Å resolution) of compound **5** in complex with human PARP-1 catalytic domain. **5** is yellow with heteroatoms being blue for nitrogen, red for oxygen, and green for fluoride. Important residues in the NI site are shown ball and stick style. (B) Homology modeled structure of compound **5** in complex with human PARP-2 catalytic domain based on the solved X-ray structure (2.8 Å resolution) of murine PARP-2. Important residues in the NI site are shown ball and stick style. (C) Close-up views of the terminal site of **5** in the AD site of PARP-1. (D) Close-up views of the terminal site of **5** in the AD site of PARP-2.

the hydrogen bond between Glu311 and Tyr431 in PARP-2. The second source of selectivity results from the replacement of Glu763 in PARP-1 with Gln308 in PARP-2. X-ray analysis shows that the side chain of Glu763 in PARP-1 is restricted by a hydrogen bond with neighbor Gln759 and Ala760 (Fig. 2A) [16], while the residue of Gln308 in PARP-2 would be mobile make a more favorable interaction with the Cl-phenyl group, since the previous study indicated the side chain of Gln763 in chicken PARP-1 appeared to be mobile and movement of this residue nicely accommodated the *p*-benzylamine substitution of inhibitors [15,17]. It is considered that the Cl-phenyl group extends into this groove containing Glu311 and

Table 2
PARP-1/2 inhibitory activities of quinoxaline analogues

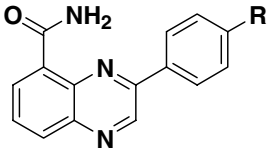

Compound	R	PARP-1 IC_{50} (nM)[a]	PARP-2 IC_{50} (nM)[a]	Selectivity PARP-2/1
9	H	131 ± 2.6	14 ± 1.3	0.11
10	Cl	33 ± 0.9	7.0 ± 2.0	0.21
11	CN	101 ± 1.8	8.0 ± 1.0	0.08
12	CF_3	118 ± 3.1	11 ± 0.9	0.09
13	OMe	71 ± 2.2	8.0 ± 0.8	0.11
14	NH_2	87 ± 3.8	9.0 ± 1.0	0.10

[a]The values are presented as means ± S.E. of three independent experiments (each experiment was triplicate).

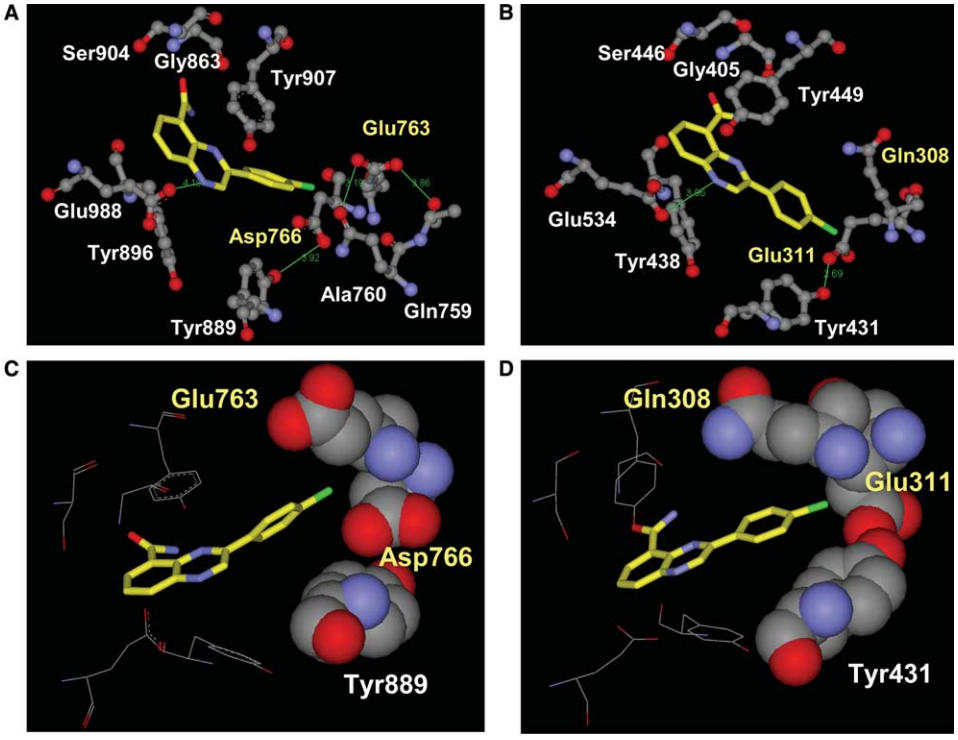

Fig. 2. (A) X-ray structure (3.0 Å resolution) of compound **10** in complex with human PARP-1 catalytic domain. **10** is yellow with heteroatoms being blue for nitrogen, red for oxygen, and green for fluoride. Important residues in the NI site are shown ball and stick style. (B) Homology modeled structure of compound **10** in complex with human PARP-2 catalytic domain based on the solved X-ray structure (2.8 Å resolution) of murine PARP-2. Important residues in the NI site are shown ball and stick style. (C) Close-up views for the binding mode of the Cl-Phenyl site of **10** in PARP-1. (D) Close-up views for the binding mode of the Cl-Phenyl site of **10** in PARP-2.

Gln308 in PARP-2 to make a more favorable interaction and may account for the increase in potency observed (Fig. 2C vs. D).

In summary, we have discovered first PARP-1 and PARP-2 selective inhibitors. SBDD study by a combination of X-ray analysis and homology modeling has revealed the distinct binding mode for the discrimination between ligands and PARP-1/2. These findings provide a new structural concept for the design of selective inhibitors for PARP-1 and PARP-2.

Acknowledgements: We express our thanks to Dr. David Barrett for his critical reading of the manuscript.

References

[1] Yu, S.W., Wang, H., Poitras, M.F., Coombs, C., Bowers, W.J., Federoff, H.J., Poirier, G.G., Dawson, T.M. and Dawson, V.L. (2002) Mediation of poly(ADP-ribose) polymerase-1 dependent cell death by apoptosis-inducing factor. Science 297, 259–263.

[2] Szabo, C. and Dawson, V.L. (1998) Role of poly(ADP-ribose)synthetase in inflammation and ischemia-reperfusion. Trends Pharmacol. Sci. 19, 287–298.
[3] Shieh, W.M., Ame, J.C., Wilson, M.V., Wang, Z.Q. and Koh, D.W. (1998) Poly(ADP-ribose)polymerase null mouse cells synthesize ADP-ribose polymerase. J. Biol. Chem. 273, 30069–30072.
[4] Ame, J.C., Rolli, V., Schreiber, V., Niedergang, C., Apiou, F., Decker, P., Muller, S., Hoger, T., Menissier-de Murcia, J. and De Murcia, G. (1999) PARP-2, a novel mammalian DNA damage-dependent poly(ADP-ribose)polymerase. J. Biol. Chem. 274, 17860–17868.
[5] (a) Ruf, A., Murcia, G. and Schulz, G.E. (1998) Inhibitor and NAD^+ binding to poly(ADP-ribose) polymerase as derived from crystal structures and homology modeling. Biochemistry 37, 3893–3900.
(b) Ruf, A., Murcia, J.M., Murcia, G.M. and Schulz, G.E. (1996) Structure of the catalytic fragment of poly(ADP-ribose) polymerase from chicken. Proc. Natl. Acad. Aci. USA 93, 7481–7485.
[6] Oliver, A.W., Ame, J.C., Roe, S.M., Good, V., DeMurcia, G. and Pearl, L.H. (2004) Crystal structure of the catalytic fragment of murine poly. Nucleic Acids Res. 32, 456–464.
[7] De Murcia, G., Schreiber, V., Molinate, M., Saulier, B., Poch, O., Masson, M., Niedergang, C. and Menissier, J. (1994) Structure and function of poly(ADP-ribose) polymerase. Mol. Cell Biochem. 138, 15–24.
[8] Kinoshita, T., Nakanishi, I., Warizaya, M., Iwashita, A., Kido, Y., Hattori, K. and Fujii, T. (2004) Inhibitor-induced structural change of the active site of human poly(ADP-ribose) polymerase. FEBS Lett. 556, 43–46.
[9] Iwashita, A., Yamazaki, S., Mihara, K., Hattori, K., Yamamoto, H., Ishida, J., Matsuoka, N. and Mutoh, S. (2004) Neuroprotective effects of a novel poly(ADP-ribose)polymerase-1 inhibitor,2-{3-[4-(4-chlorophenyl)-1-piperazinyl]propyl}-4(3H)-quinazolinone (FR255595), in an in vitro model of cell death and in mouse 1-methyl-4-phenyl-1,2,3,6-tetrahydropyridine model of Parkinson's disease. J. Pharmacol. Exp. Ther. 309, 1067–1078.
[10] Recent reviews on PARP inhibitors: Peukert, S., Schwahn, U. (2004) New inhibitors of poly(ADP-ribose)polymerase (PARP). Expert Opin. Ther. Pat. 14, 1531–1551.
[11] (a) Hattori, K., Kido, Y., Yamamoto, H., Ishida, J., Kamijo, K., Murano, K., Ohkubo, M., Kinoshita, T., Iwashita, A., Mihara, K., Yamazaki, S., Matsuoka, N., Teramura, Y. and Miyake, H. (2004) Rational approaches to discovery of orally active and brain-penetrable quinazolinone inhibitors of poly-(ADP-ribose)polymerase. J. Med. Chem. 47, 4151–4154.
(b) Iwashita, A., Mihara, K., Yamazaki, S., Matsuura, S., Ishida, J., Yamamoto, H., Hattori, K., Matsuoka, N. and Mutoh, S. (2004) A new poly(ADP-ribose) polymerase inhibitor, FR261529 [2-(4-chlorophenyl)-5-quinoxalinecarboxamide], ameliorates methamphetamine-induced dopaminergic neurotoxicity in mice. J. Pharmacol. Exp. Ther. 310, 1114–1124.
[12] Kinoshita, T., Tsutsumi, T., Maruki, R., Warizaya, M., Ishii, Y. and Fujii, T. (2004) Cloning, expression, purification, crystallization and preliminary diffraction analysis of the C-terminal catalytic domain of human poly(ADP-ribose) polymerase. Acta Crystallogr. D60, 109–111.
[13] Collaborative Computational Project, Number 4, The CCP4 suite: Programs for Protein Crystallography (1994) Acta Crystallogr. D50, 760–763.
[14] Ogata, K. and Umeyama, H. (2000) An automatic homology modeling method consisting of database searches and simulated annealing. J. Mol. Graphics Mod. 18, 258–272.
[15] (a) Canan Koch, S.S., Thoresen, L.H., Tikhe, J.G., Maegley, K.A., Almassy, R.J., Li, J., Yu, X.-H., Zook, S.E., Kumpf, R.A., Zhang, C., Boritzki, T.J., Mansour, R.N., Zhang, K.E., Ekker, A., Calabrese, C.R., Curtin, N.J., Kyle, S., Thomas, H.D., Wang, L.-Z., Calvert, A.H., Golding, B.T., Griffin, R.J., Newell, D.R., Webber, S. and Hostomsky, Z. (2002) Novel tricyclic poly(ADP-ribose)polymerase-1 inhibitors with potent anticancer chemopotentiating activity: design, synthesis, and X-ray cocrystal structure. J. Med. Chem. 45, 4961–4974.
(b) White, A.W., Almassy, R., Calvert, A.H., Curtin, N.J., Griffin, R.J., Hostomsky, Z., Maegley, K., Newell, D.R., Srinivasan, S. and Golding, B.T. (2000) Resistance-modifying agents. 9. Synthesis and biological properties of benzimidazole inhibitors of the DNA repair enzyme poly(ADP-ribose) polymerase. J. Med. Chem. 43, 4084–4097.
[16] In X-ray crystallography of **5** and PARP-1, the side chain of Glu763 in PARP-1 was also restricted by a hydrogen bond with neighbor amino acid.
[17] In murine PARP-2, the replacement of Gln308 by Lys308 was observed. The side chain of Lys308 is also not restricted; see in Ref. [6].